Radiología 64 (2022) 333–347

RADIOLOGÍA

www.elsevier.es/rx

UPDATE IN RADIOLOGY

Strengths, weaknesses, opportunities, and threat analysis of dual-energy CT in head and neck imaging☆

E. Santos Armentia[a,*], T. Martín Noguerol[b], N. Silva Priegue[a], C. Delgado Sánchez-Gracián[a], C. Trinidad López[a], R. Prada González[a]

[a] *Servicio de Radiología, Hospital Povisa, Vigo, Pontevedra, Spain*
[b] *Unidad de Resonancia Magnética, Servicio de Radiología, HT Médica, Jaén, Spain*

Received 28 March 2022; accepted 19 May 2022

KEYWORDS
Dual energy computed tomography;
Head and neck;
Strengths;
Threats;
Weaknesses;
Opportunities

Abstract Technological development of dual-energy computed tomography (DECT) can play an important role in head and neck area. Multiple innovative applications have evolved, optimizing images, achieving metallic artifact reduction, differentiating materials with better primary tumor delineation, thyroid cartilage and bone invasion. Furthermore, quantification algorithms allow measuring iodine concentration, reflecting the blood supply of a lesion indirectly.

DECT enables acquiring images with lower radiation doses and iodine intravenous contrast load to obtain the same CT values.. However, DECT uses ionizing radiation, which does not occur with MRI, and requires long post-processing times. Artifacts on iodine maps may be a potential source of pseudolesions. Besides, photon-counting CT scanners are a promising technique that may displace some DECT advantages.

A review analyzing the current status of DECT applied to head and neck imaging from the scope of strengths, weaknesses, opportunities, and threatsanalysis would be very interesting to facilitate a realistic, fact-based, data-driven look of this technique.
© 2022 SERAM. Published by Elsevier España, S.L.U. All rights reserved.

PALABRAS CLAVE
Tomografía computarizada de doble energía;
Cabeza y cuello;

Análisis de las fortalezas, oportunidades, debilidades y amenazas de la tomografía computarizada de doble energía en el diagnóstico por la imagen de la cabeza y el cuello

Resumen El desarrollo tecnológico de la tomografía computarizada de doble energía (TCDE) puede desempeñar un papel importante en el área de la cabeza y el cuello. Se han desarrollado

☆ Please cite this article as: Santos Armentia E, Martín-Noguerol T, Silva Priegue N, Delgado Sánchez-Gracián C, Trinidad López C, Prada González R. Análisis de las fortalezas, oportunidades, debilidades y amenazas de la tomografía computarizada de doble energía en el diagnóstico por la imagen de la cabeza y el cuello. Radiología. 2022;64:333–347.

* Corresponding author.
E-mail address: esantos@povisa.es (E. Santos Armentia).

2173-5107/© 2022 SERAM. Published by Elsevier España, S.L.U. All rights reserved.

Fortalezas;
Oportunidades;
Debilidades;
Amenazas

múltiples aplicaciones innovadoras, que han optimizado las imágenes, y han logrado reducir los artefactos metálicos, diferenciar los materiales con una mejor delineación del tumor primario, el cartílago tiroideo y la invasión ósea. Además, los algoritmos de cuantificación permiten medir la concentración de yodo, lo que refleja el flujo de sangre que llega a una lesión de forma indi-recta. Permite adquirir imágenes con menores dosis de radiación y menor cantidad de contrasteyodado para obtener los mismos valores de TC. Sin embargo, utiliza radiaciones ionizantes yel posprocesamiento de las imágenes consume tiempo, y los artefactos en los mapas de yodo pueden suponer una fuente potencial de seudolesiones. Además, los escáneres de TC con tecnología de recuento de fotones son una técnica prometedora que puede desplazar algunas de las ventajas de la TCDE.

Esta revisión hace un análisis de la TCED aplicada a las imágenes de cabeza y cuello desde elámbito del análisis de las fortalezas, oportunidades, debilidades y amenazas para facilitar una visión realista, basada en datos, de esta técnica.
© 2022 SERAM. Publicado por Elsevier España, S.L.U. Todos los derechos reservados.

Introduction

Head and neck is an anatomically complex region. Computed Tomography (CT) plays an important role in assessing intrinsic differences in the tissues of all the anatomical structures present in the head and neck area, translated to CT in differences in attenuation. Metallic devices in the oral cavity are frequent and may cause important artifacts that may obscure the visualization of the normal anatomy and so the pathology.[1] Moreover, some structures may be hyperdense in the basal study, such as the thyroid gland or some retained secretions,[2] or may contain calcium, hindering the identification of enhancement after intravenous contrast administration.

Dual-Energy CT (DECT) has many applications, in which the additional information provided by DECT may be a major enabler for radiologists.

In this paper, a brief reminder of the physical basis and technical background of DECT is going to be performed, followed by a Strengths, Weaknesses, Opportunities, and Threats (SWOT) analysis of this technique regarding head and neck lesions assessment.

Technical background

DECT combines the information acquired with two different energy spectra. By exploiting the differences between the two X-ray energies, mathematical algorithms may be used to obtain the following benefits: algorithms optimize the image and differentiate and quantify materials.

Image optimization

The images acquired with the two different energy spectra can be independently evaluated: low-energy level images are noisier and with higher contrast than the high-energy level images.[3]

Mathematically it is possible to mix the two datasets to yield a single ''blended'' dataset with desired features of each energy-level dataset: these are the linear-blended images representing a linear mixture of the low- and high-energy acquisitions. A weighted average (WA) linear blend of 0.3 means that 30% of the image comes from the lower energy level and 70% of the higher energy acquisition and are considered equivalent to the standard 120-kVp single energy (SECT).[4] The percentage of contribution of each dataset can be shifted, either choosing to higher-energy contribution for the increased signal-to-noise ratio (SNR) and artefact reduction or to lower-energy contribution for the improved contrast-to-noise ratio (CNR) and lesion conspicuity.[5]

By combining the high contrast and noise of the lower kiloelectron voltage (keV) and the low contrast and noise of the higher keV, non-linear blending images with high contrast and low noise may be obtained. These are the protocols of optimum contrast, optimum noise, and the optimum contrast-to-noise ratio,[6,7] which could significantly increase the contrast resolution while lowering the noise level within the image.[8]

Further, these images may also be mixed using a complex post-process to synthesize virtual monoenergetic images (VMI), creating simulated images from 40 keV to 190 keV.[9] The reconstructions performed at the lower VMI (40 keV) have high contrast and high noise, being very useful in the vascular studies,[10] and also in tumor detection and delineation (high energy images contain less noise and fewer artifacts, at the cost of iodine conspicuity). On the other hand, the higher VMIs (150 keV) have low contrast and low noise, useful to decrease the metallic artifacts and to correct the beam hardening correction[11] (Fig. 1).

Materials identification and differentiation

There are different algorithms available for material decomposition.

Two-material decomposition algorithms may differentiate two materials due to the different behaviour at two

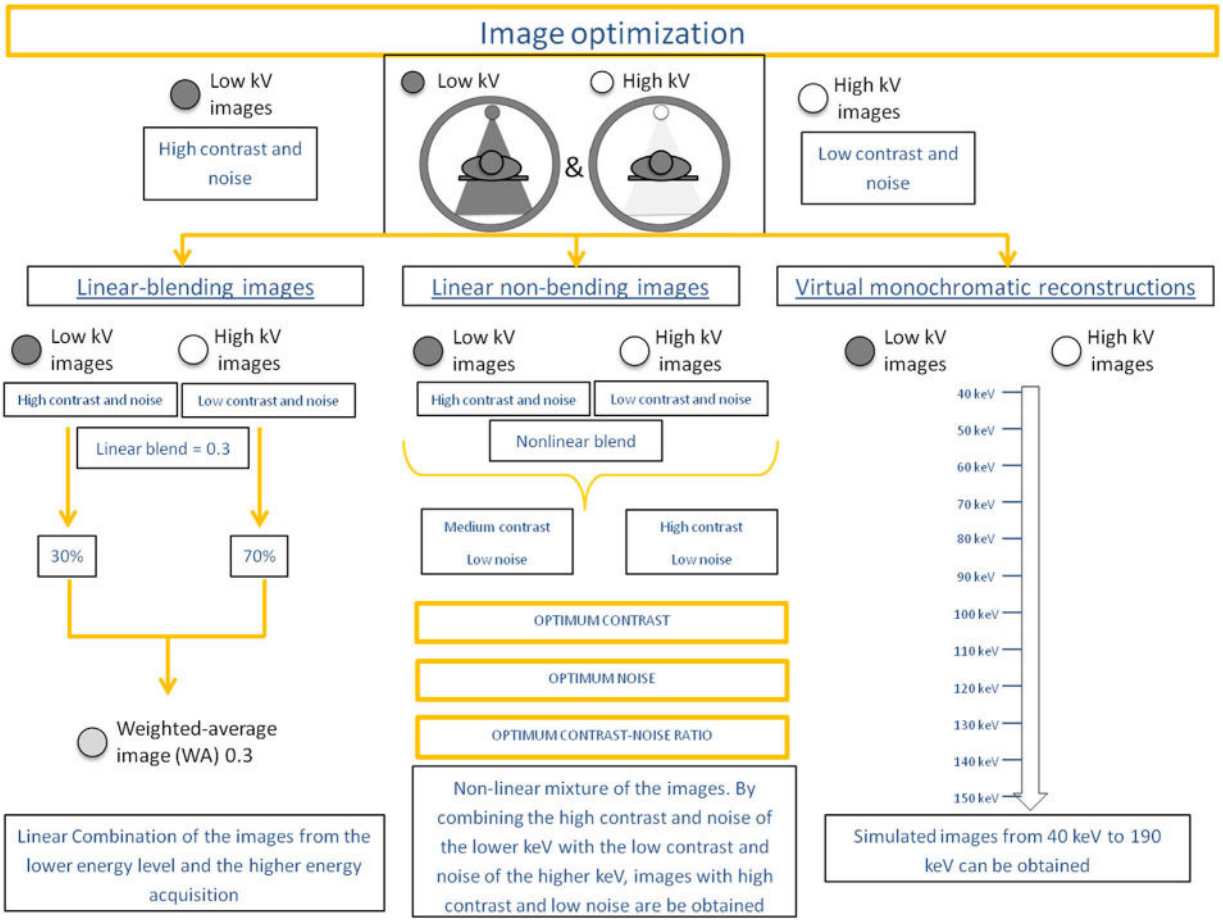

Figure 1 Scheme of the image optimization that can be performed with DECT acquisition.

distinct X-ray energy levels. I.e. water (composed of H and O, both with low atomic number, Z) and iodine (with high Z) may be distinguished, generating a water-density image in which iodine is removed (virtual non-contrast iodine image) or where iodine is highlighted (iodine map).[12]

Three-material decomposition may differentiate soft tissue, fat, and iodine, which may also provide information on attenuation and iodine.[13]

Multimaterial-decomposition algorithms have a triplet library: blood-air-fat, fat-blood-iodine, fat-iron-blood... and DECT data are tested to find the triplet that best explains the results is decomposed into the materials that correspond to the best material triplet.

These material-specific datasets are volumetric and can be evaluated as reconstructed axial images or after processing with conventional 3D applications such as multiplanar reconstruction, maximum intensity projection, and volume-rendered reformation.[14]

Quantification algorithms

Quantitative iodine concentration maps after injection of an iodinated contrast agent reflect directly the iodine concentration inside a lesion, which indirectly reflects its blood supply.[15]

SWOT analysis of dect for head and neck lesions assessment

Several studies have demonstrated the usefulness of DECT for head and neck lesions evaluation.[12,13,15] However, a systematic description of strengths, weaknesses, opportunities, and threats (SWOT) related to the use of DECT for head and neck lesions assessment would be interesting to help radiologists with the decision of acquiring and applying to specific clinical scenarios the images with dual-energy technology or with SECT (Table 1).

Strengths

There are several applications in different clinical scenarios where DECT has demonstrated its added value. These applications, commonly used in radiological clinical practice, range from image optimization to radiation dose and iodine contrast reduction and suppose the strengths of this technique for head and neck assessment nowadays.

Image optimization

As previously explained, by combining the information provided by the two energy levels, different weighted-average

Table 1 Overview of the SWOT analysis of DECT.

Strengths	Weaknesses
1. Image optimization allows to identify better:	1. Ionizing radiation and iodine contrast
- Primary tumour delineation	2. Complex physical bases, longer learning curve, and complex post-process
- Thyroid cartilage invasion	3. Pseudoenhancement at 40–70 keV
- Bone invasion	4. Material decomposition misinterpretation
- Bone marrow edema	5. Challenging to measure attenuation and to quantify the enhancement
- Parathyroid adenomas	6. Pseudolesions and hypoattenuating lesions due to beam hardening
2. Quantification algorithms	7. Incomplete masking and filtering in virtual noncalcium CT images
3. Radiation dose reduction	8. Scarce high specific applications
4. Contrast load reduction	
Opportunities	**Threads**
1. Provide further characterization of lesions	1. MRI has a higher spatial resolution with no ionizing radiation
2. May be a potential source of new biomarkers	2. PET/CT provides functional information with high sensitivity for staging head and neck malignancies
3. Could be a source of new parametric maps or source images for texture analysis or extraction of Radiomics	3. PET/MRI has a higher soft-tissue contrast of MRI compared to CT
4. Artificial intelligence may provide multi-organ segmentation and semi-automatic segmentation of the lesions	4. Photon-counting detector CT has an extremely high spatial resolution, simultaneous multienergy data acquisition, and the ability to image with and differentiate among multiple CT contrast agents

images and optimum-contrast images may be obtained, improving the visualization of certain structures.

Metal artifact reduction

Metallic hardware is frequently present in the oral cavity, causing artifacts that can negatively affect the image quality of surrounding tissues,[16] and may result in a HU shift. The extent of artifact reduction depends on the implant's location, geometry, and material composition.

VMI reconstructions of high energy levels can reduce metal artifacts and increase image quality (Fig. 2).[17,18] Tanaka et al. [18] fused DECT imaging to reduce dark band-like metal artifacts caused by dental implants and resulted in better adjacent bone diagnosis around the implants.The optimal energy levels for metal artifact reduction are generally found between 100 and 140 keV.[11,17]

Bone and calcium removal and carotid atherosclerotic plaque characterization

Bone removal algorithms may help reconstruct the angiographic studies of the supra-aortic vessels due to their ability to remove the calcified plaques to better delineate the vascular lumen.[19] DECT also offers insights into tissue characterization because the components of vulnerable atherosclerotic plaque are spectrally distinct with intrinsic contrast.[20]

Better primary tumor delineation

The evaluation of the tumor burdens and infiltration of surrounded anatomical structures is essential.[21]

Linear-blending images may optimize tumor delineation because, in images in which the percentage of the lower energy is relatively high, the delineation of head and neck tumors significantly improved (Fig. 3), demonstrated by Tawfik et al.,[22,23] Scholtz et al.,[24] and Wichmann et al.[25] Albrecht et al. evaluated the advanced application of VMI (Mono+) and found the highest tumor attenuation at 40 keV.[26]

Lam et al. recommended using a multiparametric approach to assess different structures: 65-keV VMI for a general assessment of the neck and 40-keV VMI for better tumor differentiation to the surrounding soft tissue of the surrounding soft tissue the head and neck.[27]

Thyroid cartilage invasion

Accurate detection of cartilage invasion is of great importance for the appropriate treatment choice of hypopharyngeal and laryngeal SCC.[28] On SECT imaging, the attenuation of HNSCC may be similar to non-ossified laryngeal cartilage, making it difficult to accurately distinguish subtle cartilage invasion. Tumorous cartilage has a significantly different spectral HU curve than normal non-ossified thyroid cartilage on VMIs equal to or higher than 95 keV, making it possible to differentiate them.[12,29]

Bone invasion

Dual-energy technology can differentiate between contrast material and bone with high precision because of the gap in their atomic number. Bone removal images can be used to identify small lesions near the skull base and tumor invasion. Iodine overlay images can highlight the area of tumor enhancement as different-coloured pixels, increasing visual

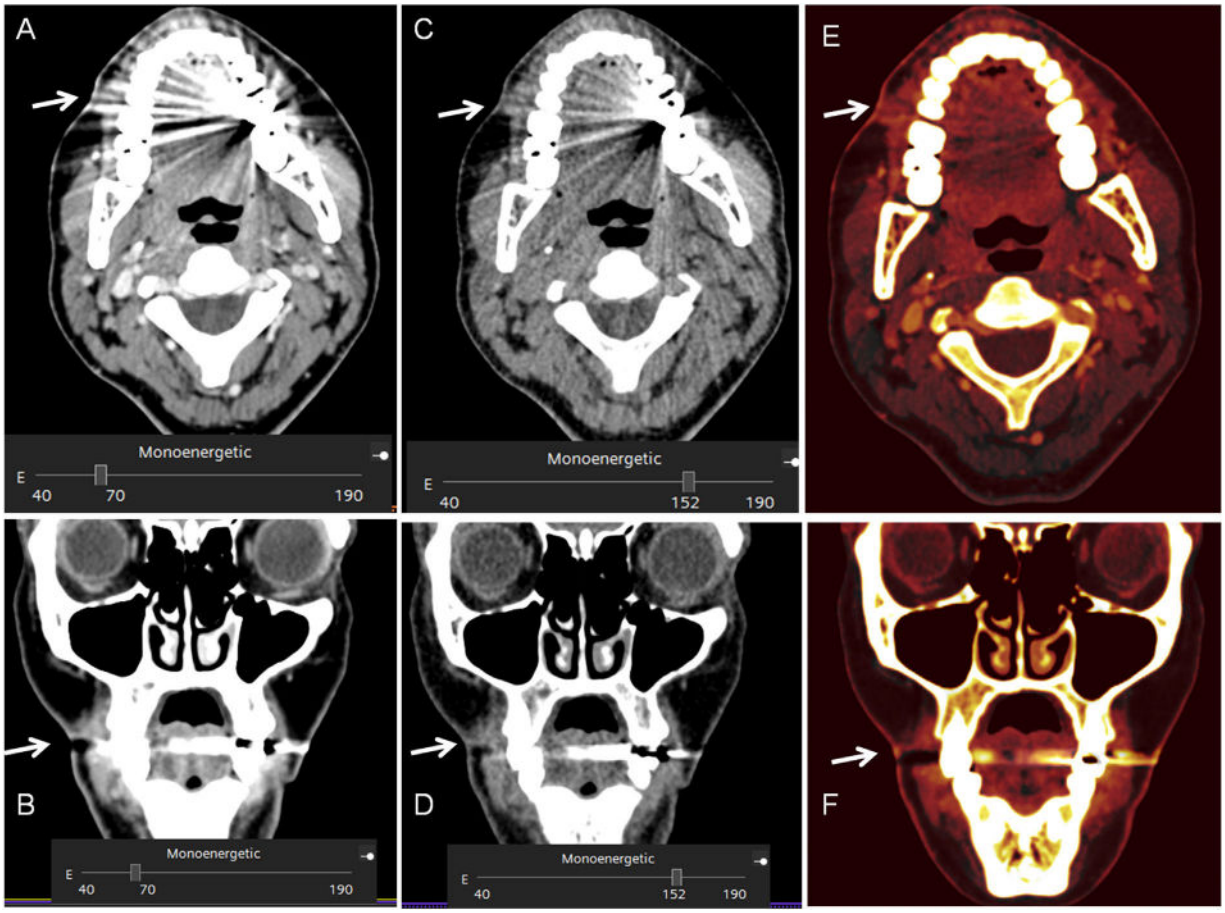

Figure 2 41-year old woman who had a facial wound in a traffic accident. 7 months later the patien presented pain with a skin depression and a produtive fistula. A. and B. 70 keV images, were the fistula and the skin thikening is difficult to spot due to the mettallic distorsion secondary to metallic reconstructions in the oral cavity. C. and D. monoenergetic reconstructions performed at 150 keV, were the reduction of the metallc artefact allow the identification of the fistulous tract. E. And F.: iodine maps allow also to visualize the fistulous tract.

lesion detection of skull base lesions and intracranial extension of extracranial tumors. Even if the CT attenuation values are similar, enhancing tumors may be differentiated from other non-enhancing or non-iodine-containing tissue such as the brain[30] (Fig. 4 and 5).

Bone marrow edema detection

The visualization of subtle bone marrow edema is the key to detect abnormalities[31] and virtual non- calcium images may help detecting this edema, highlighting the pathology.[32]

Quantification algorithms

Quantitative iodine concentration maps after injection of an iodinated contrast agent reflect directly the iodine concentration inside a lesion, which indirectly reflects the blood supply of the lesion. This may be utilized as a surrogate marker for perfusion and angiogenesis,[15,33] helping in the differential diagnosis of tumors versus benign lesions, improving the diagnostic accuracy on both diagnosis and follow-up of a specific target lesion because the rate of change of iodine concentration is related to its pathological tumor response after radiotherapy or chemotherapy treatment.

DECT iodine maps have been investigated as a dose-reduced alternative to CT perfusion measurements. An iodine distribution map is indirectly linked to perfusion because it reflects both intravascular and extravascular iodine concentrations in tissues. The intravascular component depends on regional blood volume, and the extravascular component depends on the permeability of the capillaries to contrast medium.[34] Unfortunately, the two compartments cannot be separated with this method, but by simple insertion of a region of interest (ROI), the quantitative net enhancement value, called the iodine overlay (measured in HU), can be measured.

This iodine distribution maps relies on the approximation of perfusion parameters by quantitative measurements of contrast agent concentrations with DECT acquisitions performed at strictly defined acquisition times to circumvent the need for a dynamic acquisition (Fig. 6).[35]

It has also been investigated not just the iodine concentration but the slope of the spectral curve. It has been demonstrated to be different in metastatic and non-metastatic lymph nodes.[36] For example, iodine quantification was seen significantly lower in metastatic lymph nodes than those in normal or inflammatory lymph nodes,

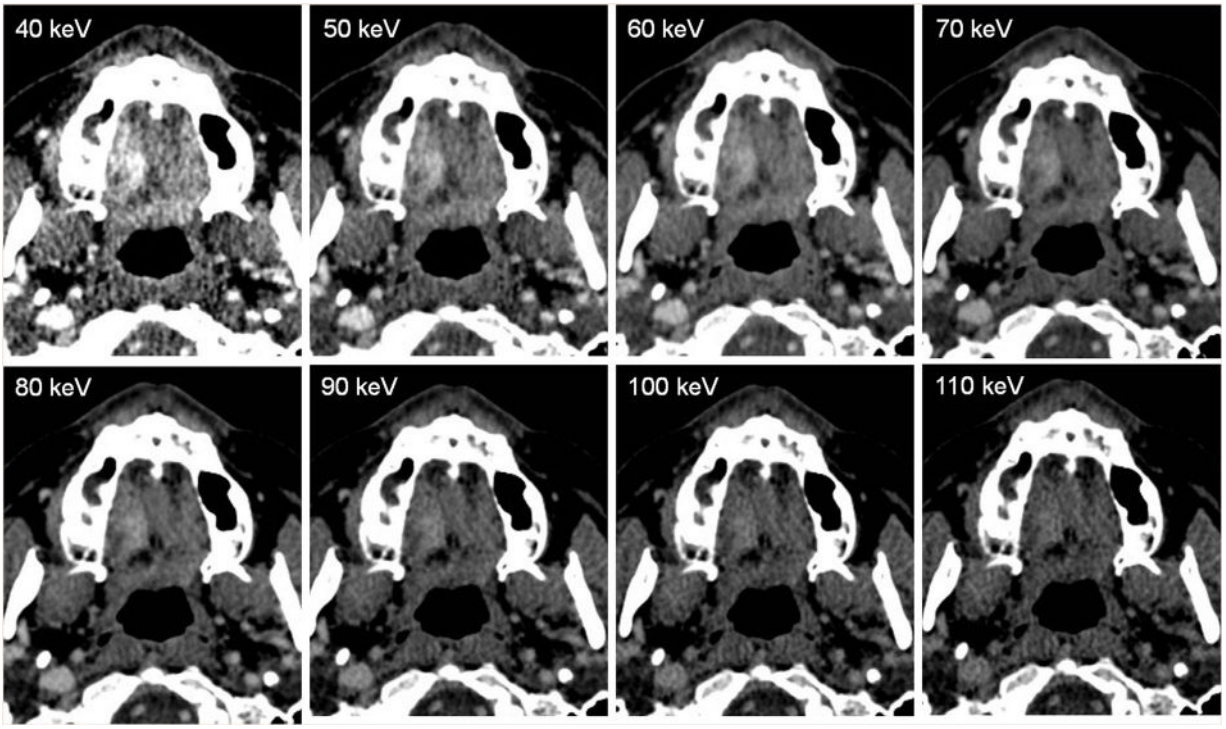

Figure 3 48-year-old woman who noticed a lump on the right side of the hard palate. On the DECT images, a soft-tissue enhancing mass is observed on the right side. Histological examination revealed an epithelial-myoepithelial carcinoma of the minor salivary glands. On the different VMI, observe that the lesion has greater contrast at the lower keV, allowing a better delimitation of the tumor at 40 keV, but the image is noisier at these lower keV. Since the keV is higher, the lesion has lower contrast, being more difficult to delineate, but the image is less noisy.

and the iodine content (measured as mg/mL) seemed more useful than the iodine overlay.[37]

Weaknesses

Because of the intrinsic DECT physical principles, one of the main weaknesses of this technique is the use of ionizing radiation. This is important compared with other radiological techniques, such as magnetic resonance imaging (MRI), in which no radiation is applied.

Technically, using DECT acquisition often involves some limited penalties compared to standard or single-energy CT. One of them is the low temporal resolution. Temporal resolution is defined as the time during which all spectral data for a given image voxel or slice is collected. For most systems, this corresponds to the time of about half a rotation and is influenced by gantry speed. Dual-source CT does not result in doubling the temporal resolution in DECT mode because a half rotation is still needed to collect the high- and low-energy projections for both imaging chains. Most vendors offer motion compensation algorithms, which are very powerful in improving effective temporal resolution.[38] For TwinBeam CT and sequential scanning, because of the delay between the high- and low-energy measurement of each given slice, the DECT temporal resolution is much poorer, resulting clinically in motion artifacts.

CT attenuation in HU is another point on DECT because it depends on two factors: the structure's effective atomic number and the energy, being challenging to quantify the attenuation at CT (in HU) in VMI. Radiologists should pay attention to the keV level when interrogating a region of interest (ROI) because the WA image of choice used in clinical practice may not provide lesion attenuation values on which most societal guidelines are based (classically SECT acquired with 120 kVp). Patel et al. suggested revised cut-off attenuation values optimized for different keV levels.[39] Attenuation keV reference tables may be a potential solution. A further difficulty is that variances in attenuation also exist among the DECT platforms, depending on the keV level and lesion type.[40]

It is described that VMIs at 40–70 keV remain susceptible to pseudoenhancement similar to that on SECT. The cause of pseudoenhancement is likely multifactorial, being a combination of beam hardening, partial volume averaging, scatter, or crosstalk,[41] and has been described when lesions are scanned at peak parenchymal enhancement, classically described in the evaluation of small renal cystic lesions.[42]

High-energy VMC imaging mitigates metal artifacts by reducing beam hardening, but images cannot alleviate photon starvation artifacts. This means that the artifact-reducing capability is affected by the type of alloy and the device's size because of their different interaction with x-ray photons. This explains why cobalt-chrome metallic devices are less amenable to artifact reduction because the cause of the artifact is photon starvation[41] (Fig. 7).

Material decomposition makes binary discrimination of materials, and the presence of another material may result in erroneous representation images created with that mate-

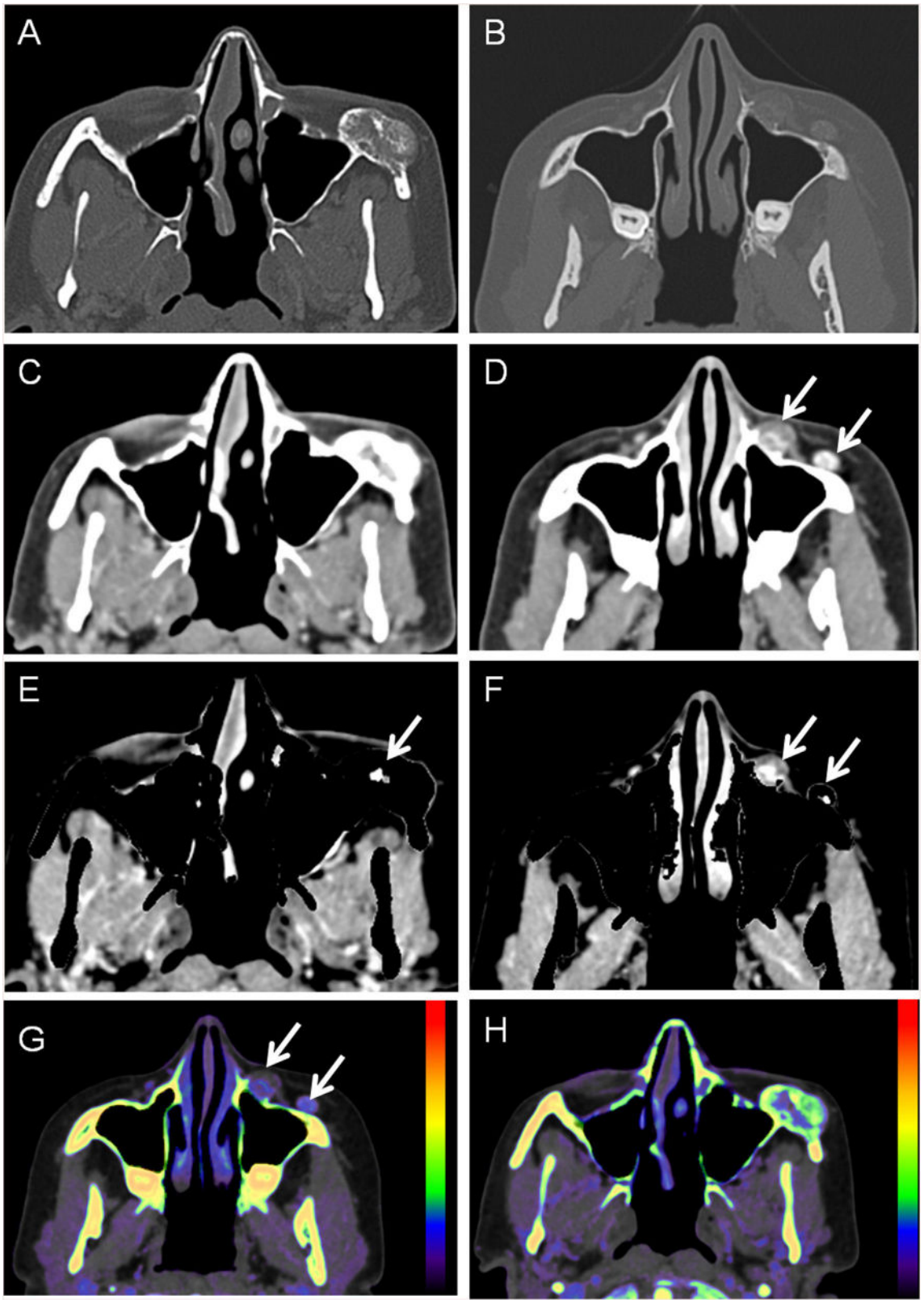

Figure 4 46- year old woman with slow growing mass on the left malar region. A. and B. Bone window showing a excrecent lesion. C. and D. Soft tissue window showing a small soft- tissue mass (arrows) but on C no enhancement can be visualized. E. and F. Bone removal images allow to visualize enhancement both inside the bone lesion (arrow on E) and on the adjacent sof tissues (F). G. and H. Effective z images, were different Z numbers are mapped to different colors, showing enhancement inside the lesion. After surgical resection it was an vascular venous malformation.

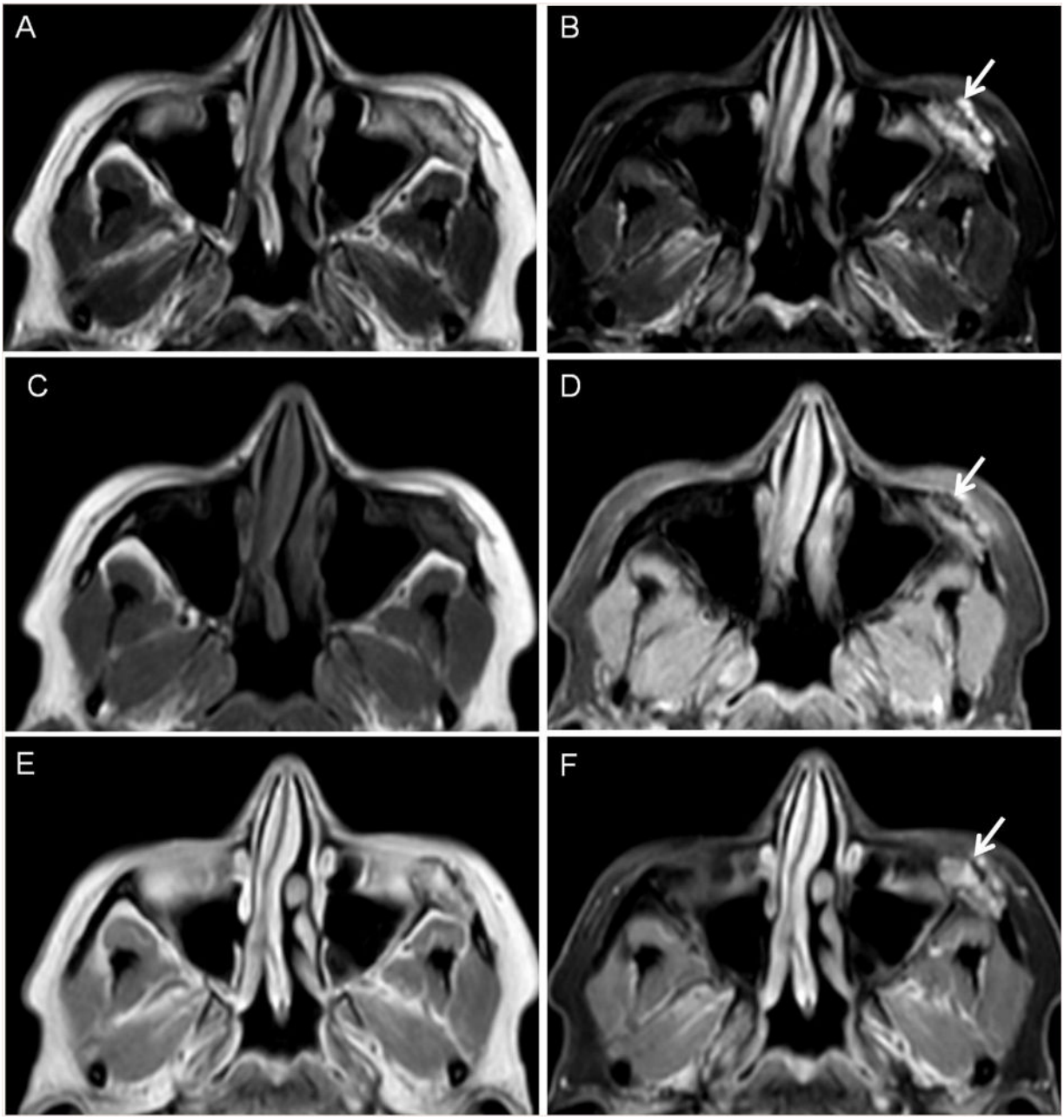

Figure 5 Facial MRI of patient of Fig. 3. A. T2, B. T2 FatSat, C. T1, D. T1 FatSat, E. T1 with contrast and F. T1 FatSat after intraveous contrast with contrast allowing to detect contrast enhancement inside the bone lesion corresponding to a vascular venous malformation.

rial decomposition technique. This explains why calcium- and bone-containing voxels can be visualized on iodine maps and can be interpreted as an iodine-containing material. This also happens with highly attenuating items, such as metallic devices, pacemakers, and stents that can appear to be hyperattenuating on iodine maps, although they do not contain iodine. Because of this, material decomposition images should only be evaluated for the material pairs to which they correspond (Fig. 8).

It is also challenging to determine cutoff values to detect enhancement. There is insufficient literature and the values can vary according to the DECT platform used, as described by Patel et al., who demonstrated the need for platform-specific thresholds and found that irrespective of platform, an absolute value of 1.5 mg/mL can allow vascular lesions to be discerned from nonvascular lesions.[43] The authors also demonstrated that a relative or normalized measurement obtained by calculating the ratio of lesion-to-aorta iodine concentration reduces interplatform variability and improves diagnostic performance interpatient variability between injected iodine loads.

Artifacts on iodine maps inside benign lesions due to image noise, scatter, or imaging parameters may be a potential source of pseudolesions. They can appear as speckles of

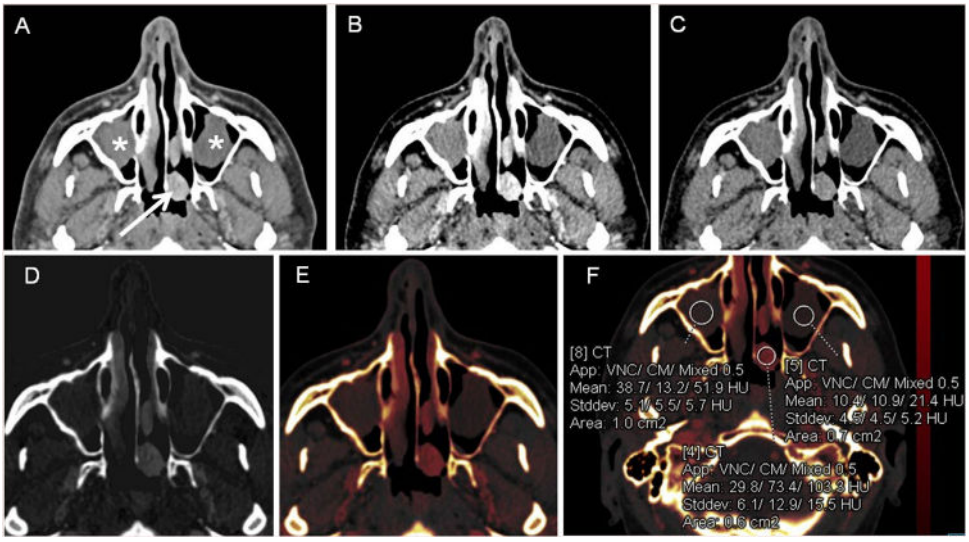

Figure 6 83-year-old woman with osteonecrosis on the first and second quadrant, with lytic lesions with osseous fragmentation involving the alveolar ridge (white arrows) A. Panoramic image reconstruction, B. WA image with strong artifact due to the presence of metallic devices in the oral cavity. C. VMIs show a significant reduction of artifact in the higher monoenergetic reconstructions, but it does not disappear entirely. This is because VMI can alleviate beam hardening artifact but cannot alleviate photon starvation artifacts. Artifact-reducing capability depends on the type of alloy and prosthesis size because of differences in their interaction with X-ray photons.

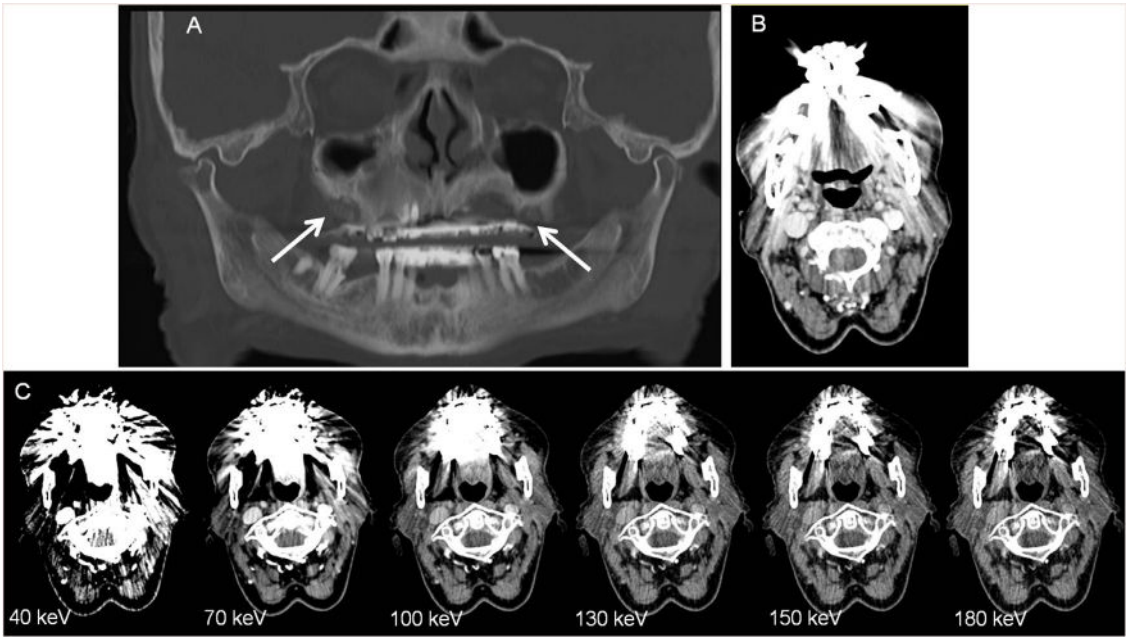

Figure 7 49-year-old man with sinonasal polyposis. A. On the WA image, partial occupation of both maxillary sinuses and the left nasal cavity is observed. The density is slightly denser on the nasal cavity lesion (arrow) than inside the maxillary sinuses (asterisk). B. 80 kV and C. 140 kV acquisitions, where this different behavior is more evident, being denser the occupying lesion of the left nasal fossa on the 80 kV acquisition. D. Ionide map and E.: colour-coded Iodine map showing higher signal inside the lesion of the nasal fossa, making manifest the enhancement inside the lesion of the nasal fossa. F.: quantitative iodine concentration map comparing both sides revealed enhancement of the nasal fossa lesion (corresponding to olfactory neuroblastoma after resection) and absence of enhancement of the maxillary sinuses content.

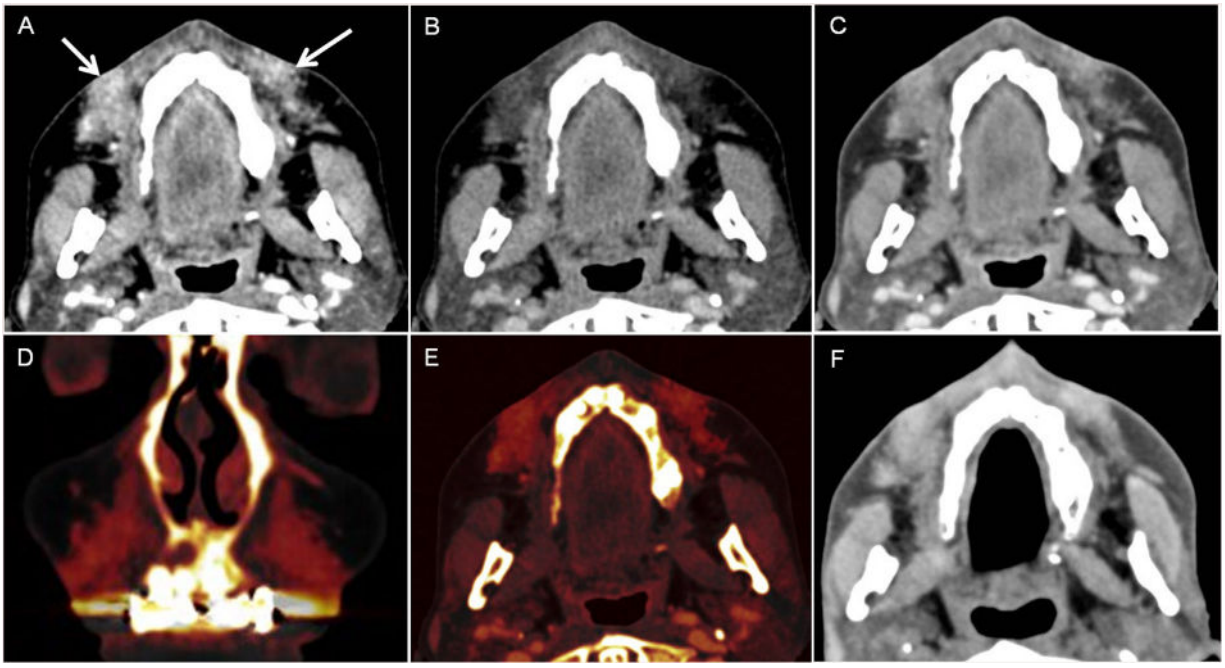

Figure 8 A pitfall of material decomposition images. A 51-year-old woman with facial pain. Facial CT after iodine contrast administration (A–E). In the nasolabial region, a bad-defined infiltration of the fat is seen, due to injected cosmetic fillers. A. 80 kVp, B. 140 kVp and C. 0.6 WA image. Iodine maps in D. coronal and E. axial, in which this material is hyperintense, simulating contrast enhancement, but corresponding to an artifactual image in material differentiation images because materials other than iodine, such as calcium, can appear to be hyperattenuating although they do not contain iodine. F. Facial CT was performed 3 years later without intravenous contrast administration on SECT, in which the density is similar to the WA image, demonstrating the lack of contrast enhancement.

color, which can be confused with the presence of iodine in the lesion reflecting enhancement.[44] Artifactual defects, most likely because of photon starvation, can also mimic hypoattenuating lesions.[45] Findings on MD iodine CT images should be correlated with those on VMC CT images and those from other examinations. If doubt persists, further evaluation with contrast-enhanced MRI may be needed.

Incomplete masking and filtering in virtual noncalcium CT images can limit assessment of regions of less than 2 mm in dense cortical bone, including subcortical areas and vertebrae less than 4 mm in height or more than 50% sclerosis and gas on virtual noncalcium CT images.[46]

Further noise optimization is necessary for material decomposition images to improve their image quality in all dual-energy approaches. Technical limitations include artifacts at dual-energy post-processing in regions of photon starvation where there are inadequate low-kilovoltage data to characterize materials. These artifacts may appear in areas of overlying metal or in highly attenuating parts of the body such as the shoulders, where there may not be adequate x-ray penetration at 80 kV. Recently, some algorithms have been published to achieve effective noise suppression.[47]

Other limitations of DECT are the costs. On the one hand, specific software is needed to perform the post-process of these examinations. In addition, depending on the type of scanner and the reconstructions, DECT examinations may require additional time for image processing at the CT console spectral CT technique and applications, compared with SECT acquisitions. On the other hand, the costs derived on the possible change of the organization on CT department to maintain productivity, particularly in settings where the scanner is operating at full or near full capacity[13] because of these reasons: the generated series provide a significantly higher number of images, and post-processing methods are time-consuming: linear-blending, linear-non blending, VMI, iodine quantification, bone subtraction... and in some patients several post-process methods are helpful in the evaluation of one single lesion, i.e., when studying an oral lesion, lower energy levels could give more information about lesion enhancement, but more metallic artifact will be present, so the radiologist should evaluate one issue at one monoenergetic imaging and vary the monoenergetic level to decrease the metallic artifact and be able to delineate the tumor.

Besides, this technique has a complex physical basis, which makes radiologists need a learning curve to become familiar with image interpretation.

The consequences of all these factors are a substantial increase the radiologists' workload, which could hinder the use of dual-energy CT imaging in daily routine. However, manufacturers are working to improve the automation of post-processing workflows.[30]

Opportunities

The further characterization of lesions provided by DECT (bone and calcium-subtraction, virtual monochromatic imaging, material characterization...) allow a multipara-

metric evaluation of head and neck lesions in just one acquisition[27] and an approach to functional imaging.[48] This may have implications for assessing prognosis and treatment monitoring, enabling a full quantification of the primary tumor and neck metastases.[37] In this way, DECT could be a potential source of new biomarkers[49,50] within interesting applications in radiobiology, and maybe in the future potential applications in response evaluation criteria in solid tumors (RECIST) could be implemented.

Uhrig et al. evaluated the feasibility of semi-automatic RECIST evaluation with supplementary iodine uptake quantification in melanoma metastases treated with the BRAF inhibitor vemurafenib and found that it enabled objective, easy and fast parameterization of tumor size and contrast medium uptake, thus providing two complementary pieces of information for response monitoring applicable in daily routine.[51]

Modified Choi criteria, which measure hypervascular tumors, have been proposed as alternatives to RECIST. The Choi criteria define a partial response by either a 10% reduction in size or a 15% reduction in density during the portal venous contrast phase.[52] Kim et al. demonstrated that DECT may serve as a useful tool for response evaluation after anti-angiogenic treatment in non-small cell lung cancer patients by providing information on the extent of tumor nodules and lymph nodes enhancement, which can be accomplished without obtaining non-enhanced images, by assessing intratumoral changes comparing DECT (based on Choi's criteria) to RECIST criteria.[53] Swiecicki et al. demonstrated that the Choi criteria appear to identify better patients responding to therapy with the anti-angiogenic tyrosine kinase inhibitor axitinib versus RECIST v1.0,[54] so DECT may provide a great opportunity in judging response to axitinib therapy in unresectable recurrent or distant metastatic head and neck squamous cell carcinoma.

In the last few years, artificial intelligence (AI) has been increasing and improving. In this respect, AI with DECT could help make automatic multi-organ segmentation[55] and semi-automatic segmentation of the lesions[56]; and may streamline the post-processing workflow, helping to manage all the enormous quantity of information and data which cannot be manually processed. It also may create texture-analyses maps, may be a source of new parametric maps or source images for texture analysis or extraction of radiomics.[56,57]

Seidler et al. used machine learning assisted-texture analysis of VMI datasets from DECT to differentiate metastatic HNSCC lymph nodes from lymphoma, inflammatory, or normal lymph nodes and found an accuracy, sensitivity, specificity, PPV, and NPV for correctly classifying a lymph node as malignant (i.e. metastatic HNSCC or lymphoma) versus benign were 92%, 91%, 93%, 95%, 87%, respectively.[57]

An important opportunity of DECT is radiation dose. A common misconception is that the radiation dose increases with DECT due to the acquisition of data at both high and low kilovoltage levels. In reality, with existing systems, the radiation dose is split between the data acquired at low and high kilovoltage settings such that the overall radiation dose delivered in a comparable acquisition typically is maintained with DECT approaches. Zhu et al., on a 10-year-old child-based phantom, compared the CTDIvol of SECT and DECT[58] and found no significant alteration in image quality between SECT and DECT, but the amount of dose in SECT was significantly more than DECT. Tawfik et al. demonstrated that DECT of the head and neck either for diagnostic or research purposes is comparable with a standard 120-kVp acquisition even when the radiate dose is lower by 12%, with the bonus of providing multiple additional datasets that may provide valuable additional information.[59] Suntharalingam et al. described that head and neck imaging with third-generation DECT could reduce radiation dose by half compared to SECT while maintaining excellent image quality.[60] This gains importance when scanning children or oncologic patients in which several CTs should be performed.[61]

It should not be forgotten that virtual unenhanced images obviate the need of scanning the patient without contrast administration because enhancing lesions can be differentiated from calcification and other high-attenuation lesions

Another advantage of DECT is that it allows decreasing intravenous contrast material load needed to obtain the same CT numbers. Reducing iodine load decreases the risk of contrast-induced nephropathy, being beneficial in terms of safety and costs.[62] At lower X-ray energy levels, attenuation of iodine contrast increases as the energy level approaches the K-edge of iodine (33.2 keV), allowing for iodine intravenous contrast reduction to obtain the same CT-values.[63] Several authors have reported iodine dose reductions of up to 70% with DECT for aortic and coronary CTA while maintaining objective image quality.[64–68] For head and neck CT-angiography, Zhao et al. described a reduction in iodine load and radiation dose in head-neck CT angiography, enhancing signal intensity and maintaining image quality by injecting 50 mL of 270 mg I/mL.[69] Optimal scan protocol and to which extent varied per vendor.[63]

Threats

Several external threats hinder a deeper implementation of DECT in common clinical and radiological practice. From a practical point of view, three main imaging modalities compete directly with DECT. SECT equipment, PET/TC, and MRI. SECT equipment are cheaper, and all the acquisition and post-processing are faster than DECT. They are widely available, so findings are globally extended with less physics complexity, being the state-of-the-art imaging of head and neck imaging.[70]

PET/CT provides functional information with high sensitivity for staging head and neck malignancies, diagnosing tumor recurrence, helping to direct biopsy, detecting the unknown primary tumor site.[71] Nowadays, this technique is more available than DECT. PET/MRI has a higher soft-tissue contrast of MRI compared to CT. This is especially advantageous when imaging the complex anatomical structures that reside within the head and neck, and is preferred in patients who have suspected perineural disease or have primary tumors that are at high risk for perineural tumor spread, such as salivary gland neoplasms, orbital tumors, and skin cancer, and not forgetting it allows for a significant reduction in radiation dose to the patient compared to PET/CT.[72]

The biggest threat of DECT in the head and neck area is the MRI, because for many reasons: MRI does not use

ionizing radiation, it is widely available and incorporated into de daily clinical practice, and it provides higher tissular resolution and physiological information thanks to the use of diffusion and perfusion techniques. Iodine contrast is not used but gadolinium, reducing the risk of contrast material-induced nephropathy. However, it is not to forget the potential risk of nephrogenic systemic fibrosis that may occur with gadolinium-based contrast material.[73] It should be commented that in many centres, the follow-up of patients with head and neck tumors is performed using CT.[74]

Photon-counting detector CT is an emerging technology that has shown tremendous progress in the last decade. It uses an X-ray detector with improved energy-resolving power with substantial benefits, which include reduced electronic noise, increased contrast-to-noise ratio with iodinated contrast material and radiation dose efficiency, reduced beam-hardening and metal artifacts, extremely high spatial resolution, simultaneous multi-energy data acquisition, and the ability to image with and differentiate among multiple CT contrast agents.[75] so this technology could be a great threat to DECT.

Conclusions

DECT may help radiologists enhance CT's confidence when evaluating head and neck pathology by decreasing metal or beam-hardening artifacts, increasing iodine contrast-to-noise ratio, improving image quality by significantly reducing noise with the best mixture of the high- and the low-kV dataset, and providing material-specific information. CT can be acquired with a lower radiation dose and a lower iodine contrast load, but it can be time-consuming, and some technical improvements may be resolved.

Funding

No funding was received for this study.

Ethics approval

The hospital ethical committee approved this paper.

All procedures performed in studies involving human participants were following the ethical standards of the institutional research committee and with the 1964 Helsinki declaration and its later amendments or comparable ethical standards.

Consent to participate

Due to the retrospective nature of this review and the anonymization of the images, the local ethical committee waived the need for written consent informed.

Key points

- Review the current situation of Dual Energy CT (DECT) on head and neck imaging.
- To perform a strengths, weakness, opportunities, and threats (SWOT) analysis of DECT in this anatomic region.

Authorship

1. Responsible for study integrity: E.S.A., T.M.N.
2. Study conception: E.S.A., T.M.N.
3. Study design: E.S.A., T.M.N.
4. Data acquisition: E.S.A., N.S.P., C.D.S.-G., C.T. L., R.P.G.
5. Data analysis and interpretation: E.S.A., N.S.P., C.D.S.-G., C.T. L., R.P.G.
6. Statistical processing: N.A.
7. Literature search: E.S.A., T.M.N.
8. Drafting of the manuscript: E.S.A., T.M.N.
9. Critical review of the manuscript with intellectually significant contributions: E.S.A., TT.M.N., N.S.P., C.D.S.-G., C.T. L., R.P.G.
10. Approval of the final version: E.S.A., TT.M.N., N.S.P., C.D.S.-G., C.T. L., R.P.G.

Conflict of interest

The authors declare that they have no conflict of interest.

Consent for publication

Not applicable.

Acknowledgments

We would like to acknowledge to Ph.D. José María García Santos who provided insight, expertise, and comments that greatly improved the manuscript.

References

1. Wippold FJ. Head and neck imaging: the role of CT and MRI. J Mag Res Imag. 2007;25:453–65.
2. Imanishi Y, Ehara N, Mori J, Shimokawa M, Sakuyama K, Ishikawa T, et al. Measurement of thyroid Iodine by CT. J Comput Assist Tomog. 1991;15:287–90.
3. Gnannt R, Winklehner A, Goetti R, Schmidt B, Kollias S, Alkadhi H. Low kilovoltage CT of the neck with 70 kVp: comparison with a standard protocol. Am J Neuroradiol. 2012;33:1014–9.
4. Holmes DR, Fletcher JG, Apel A, Huprich JE, Siddiki H, Hough DM, et al. Evaluation of non-lineal blending in dual-energy computed tomography. Eur J Radiol. 2008;68:409–13.
5. Johnson TRC. Dual-energy CT: general principles. AJR Am J Roentgenol. 2012;199 5 Suppl:S3–8.
6. Eusemann C, Holmes IIIDR, Schmidt B, Flo h TG, Robb R, McCollough C, et al. Dual energy CT: how to best blend both energies in one fused image? Mededical Imaging 2008: visualization, image-guided procedures, and modeling. SPIE. 2008:691803.
7. Vogl TJ, Schulz B, Bauer RW, Stöver T, Sader R, Tawfik AM. Dual-energy CT applications in head and neck imaging. AJR Am J Roentgenol. 2012;199 5 Suppl:S34–9.
8. Li S, Wang C, Jiang X, Xu G. Effects of dual-energy CT with nonlineal blending on abdominal CT angiography. Korean J Radiol. 2014;15:430–8.

9. McCollough CH, Leng S, Yu L, Fletcher JG. Dual- and multi-energy CT: principles, technical approaches, and clinical applications. Radiology. 2015;276:637–53.
10. De Zordo T, von Lutterotti K, Dejaco C, Soegner PF, Frank R, Aigner F, et al. Comparison of image quality and radiation dose of different pulmonary CTA protocols on a 128-slice CT: high-pitch dual source CT, dual energy CT and conventional spiral CT. Eur Radiol. 2012;22:279–86.
11. Wang Y, Qian B, Li B, Qin G, Zhou Z, Qiu Y, et al. Metal artifacts reduction using monochromatic images from spectral CT: evaluation of pedicle screws in patients with scoliosis. Eur J Radiol. 2013;82(8).
12. Forghani R. Advanced dual-energy CT for head and neck cancer imaging. Exp Rev Anticancer Ther. 2015;15:489–501.
13. Pérez-Lara A, Forghani R. Spectral computed tomography: technique and applications for head and neck cancer. Magn Reson Imag Clin N Am. 2018;26:1–17.
14. Godoy MCB, Naidich DP, Marchiori E, Assadourian B, Leidecker C, Schmidt B, et al. Basic principles and posprocessing techniques of dual-energy CT: illustrated by selected congenital abnormalities of the thorax. J Thor Imag. 2009;24:152–9.
15. Sadick M, Schoenberg SO, Hoermann K, Sadick H. Current oncologic concepts and emerging techniques for imaging of head and neck squamous cell cancer. GMS Curr Top Otorhinolaryngol Head Neck Surg. 2012;11:Doc08.
16. Barrett JF, Keat N. Artifacts in CT: recognition and avoidance. Radiographics. 2004;24:1679–91.
17. Zhou C, Zhao YE, Luo S, Shi H, Li L, Zheng L, et al. Monoenergetic imaging of dual-energy CT reduces artifacts from implanted metal orthopedic devices in patients with factures. Acad Radiol. 2011;18:1252–7.
18. Tanaka R, Hayashi T, Ike M, Noto Y, Goto TK. Reduction of dark-band-like metal artifacts caused by dental implant bodies using hypothetical monoenergetic imaging after dual-energy computed tomography. Oral Surg Oral Med Oral Pathol Oral Radiol. 2013;115:833–8.
19. Mannil M, Ramachandran J, Vittoria de Martini I, Wegener S, Schmidt B, Flo h T, et al. Modified dual-energy algorithm for calcified plaque removal: evaluation in carotid computed tomography angiography and comparison with digital subtraction angiography. Invest Radiol. 2017;52:680–5.
20. Zainon R, Ronaldson JP, Janmale T, Scott NJ, Buckenham TM, Butler APH, et al. Spectral CT of carotid atherosclerotic plaque: comparison with histology. Eur Radiol. 2012; 22:2581–8.
21. Shah JP, Gil Z. Current concepts in management of oral cancer. Surgery. Oral Oncol. 2009;45:394–401.
22. Macari M, Spieler B, Kim D, Graser A, Megibow AJ, Babb J, et al. Dual-source dual-energy MDCT of pancreatic adenocarcinoma: initial observations with data generated at 80 kVp and at simulated weighted-average 120 kVp. Am J Roentgenol. 2010;194:27–32.
23. Tawfik AM, Kerl JM, Bauer RW, Nour-Eldin NE, Naguib NNN, Vogl TJ, et al. Dual-energy CT of head and neck cancer: average weighting of low-and high-voltage acquisitions to improve lesion delineation and image quality-initial clinical experience. Invest Radiol. 2012;47:306–11.
24. Scholtz JE, Hüsers K, Kaup M, Albrecht M, Schulz B, Frellesen C, et al. Non-lineal image blending improves visualization of head and neck primary squamous cell carcinoma compared to lineal blending in dual-energy CT. Clin Radiol. 2015;70: 168–75.
25. Wichmann JL, Nöske E-M, Kraft J, Burck I, Wagenblast J, Eckardt A, et al. Virtual monoenergetic dual-energy computed tomography: optimization of kiloelectron volt settings in head and neck cancer. Invest Radiol. 2014;49:735–41.
26. Albrecht MH, Scholtz JE, Kraft J, Bauer RW, Kaup M, Dewes P, et al. Assessment of an advanced monoenergetic reconstruction technique in dual-energy computed tomography of head and neck cancer. Eur Radiol. 2015;25:2493–501.
27. Lam S, Gupta R, Kelly H, Curtin HD, Forghani R. Multiparametric evaluation of head and neck squamous cell carcinoma using a single-source dual-energy CT with fast kVp switching: state of the art. Cancers. 2015;7:2201–16.
28. Kuno H, Onaya H, Iwata R, Kobayashi T, Fujii S, Hayashi R, et al. Evaluation of cartilage invasion by laryngeal and hypopharyngeal squamous cell carcinoma with dual-energy CT. Radiology. 2012;265:488–96.
29. Kuno H, Sakamaki K, Fujii S, Sekiya K, Otani K, Hayashi R, et al. Comparison of MR imaging and dual-energy CT for the evaluation of cartilage invasion by laryngeal and hypopharyngeal squamous cell carcinoma. Am J Neuroradiol. 2018;39:524–31.
30. Potter CA, Sodickson AD. Dual-energy CT in emergency neuroimaging: added value and novel applications. Radiographics. 2016;36:2186–98.
31. Gosangi B, Mandell JC, Weaver MJ, Uyeda JW, Smith SE, Sodickson AD, et al. Bone marrow edema at dual-energy CT: a game changer in the Emergency Department. Radiographics. 2020;40:859–74.
32. Roele ED, Timmer VCML, Vaassen LAA, van Kroonenburgh AMJL, Postma AA. Dual-energy CT in head and neck imaging. Curr Radiol Rep. 2017;5:19.
33. Schmid-Bindert G, Henzler T, Chu TQ, Meyer M, Nance JW Jr, Schoepf UJ, et al. Functional imaging of lung cancer using dual energy CT: how does iodine related attenuation correlate with standardized uptake value of 18FDG-PET-CT? Eur Radiol. 2012;221:93–103.
34. Miles KA. Tumour angiogenesis and its relation to contrast enhancement on computed tomography: a review. Eur J Radiol. 1999;30:198–205.
35. Skornitzke S, Fritz F, Mayer P, Koell M, Hansen J, Pahn G, et al. Dual-energy CT iodine maps as an alternative quantitative imaging biomarker to abdominal CT perfusion: determination of appropriate trigger delays for acquisition using bolo tracking. Br J Radiol. 2018;91:20170351.
36. Liang H, Li A, Li Y, Cheng H, Zhao Q, Li J, et al. A retrospective study of dual-energy CT for clinical detecting of metastatic cervical lymph nodes in laryngeal and hypopharyngeal squamous cell carcinoma. Acta Otolaryngol. 2015;135: 722–8.
37. Tawfik AM, Razek AA, Kerl JM, Nour-Eldin NE, Bauer R, Vogl TJ. Comparison of dual-energy CT-derived iodine content and iodine overlay of normal, inflammatory and metastatic squamous cell carcinoma cervical lymph nodes. Eur Radiol. 2014;24: 574–80.
38. Forghani R, de Man B, Gupta R. Dual-energy computed tomography: physical principles, approaches to scanning, usage, and implementation: part 2. Vol. 27. Neur Clin N Am. 2017;27:385–400.
39. Patel BN, Farjat A, Schabel C, Duvnjak P, Mileto A, Ramirez-Giraldo JC, et al. Energy-specific optimization of attenuation thresholds for low-energy virtual monoenergetic images in renal lesion evaluation. Am J Roentgenol. 2018; 210:W205–17.
40. Mileto A, Barina A, Marin D, Stinnett SS, Choudhury KR, Wilson JM, et al. Virtual monochromatic images from dual-energy multidetector CT: variance in CT numbers from the same lesion between single-source projection-based and dual-

source image-based implementations. Radiology. 2016;279: 269–77.
41. Parakh A, Lennartz S, An C, Rajiah P, Yeh BM, Simeone FJ, et al. Dual-energy CT images: pearls and pitfalls. Radiographics. 2021;41:98–119.
42. Mileto A, Nelson RC, Samei E, Jaffe TA, Paulson EK, Barina A, et al. Impact of dual-energy multi-detector row CT with virtual monochromatic imaging on renal cyst pseudoenhancement: in vitro and in vivo study. Radiology. 2014;272:767–76.
43. Patel BN, Vernuccio F, Meyer M, Godwin B, Rosenberg M, Rudnick N, et al. Dual-energy CT material density iodine quantification for distinguishing vascular from nonvascular renal lesions: normalization reduces intermanufacturer threshold variability. Am J Roentgenol. 2019;212:366–76.
44. Wortman JR, Sodickson AD. Pearls, pitfalls, and problems in dual-energy computed tomography imaging of the body. Radiol Clin North Am. 2018;56:625–40.
45. Parakh A, Baliyan V, Sahani DV. Dual-energy CT in focal and diffuse liver disease. Curr Radiol Rep. 2017;5:1–14.
46. Biondi M, Vanzi E, de Otto G, Banci Buonamici F, Belmonte GM, Mazzoni LN, et al. Water/cortical bone decomposition: a new approach in dual energy CT imaging for bone marrow oedema detection. A feasibility study. Phys Medica. 2016; 32:1712–6.
47. Jiang Y, Zhang X, Sheng K, Niu T, Xue Y, Lyu Q, et al. Noise suppression in image-domain multi-material decomposition for dual-energy CT. IEEE Trans Biomed Eng. 2020;67: 523–35.
48. Fornaro J, Leschka S, Hibbeln D, Butler A, Anderson N, Pache G, et al. Dual- and multi-energy CT: approach to functional imaging. Insights Imaging. 2011;2:149–59.
49. Kay FU, Oz OK, Abbara S, Barbosa EJM, Agarwal PP, Rajiah P. Translation of quantitative imaging biomarkers into clinical chest CT. Radiographics. 2019;39:957–76.
50. Manoharan D, Netaji A, Das CJ, Sharma S. Iodine parameters in triple-bolus dual-energy CT correlate with perfusion CT biomarkers of angiogenesis in renal cell carcinoma. Am J Roentgenol. 2020;214:808–16.
51. Uhrig M, Sedlmair M, Schlemmer HP, Hassel JC, Ganten M. Monitoring targeted therapy using dual-energy CT: semi-automatic RECIST plus supplementary functional information by quantifying iodine uptake of melanoma metastases. Cancer Imaging. 2013;13:306–13.
52. Weng Z, Ertle J, Zheng S, Lauenstein T, Mueller S, Bockisch A, et al. Choi criteria are superior in evaluating tumor response in patients treated with transarterial radioembolization for hepatocellular carcinoma. Oncol Lett. 2013;6: 1707–12.
53. Kim YN, Lee HY, Lee KS, Seo JB, Chung MJ, Ahn MJ, et al. Dual-energy CT in patients treated with anti-angiogenic agents for non-small cell lung cancer: new method of monitoring tumor response? Korean J Radiol. 2012;13:702–10.
54. Bellile E, Srinivasan A, Worden FP, Swiecicki PL, Dickerson E. Alternative imaging response criteria with the use of axitinib in head and neck cancer: an exploratory analysis utilizing the choi criteria. Otolaryngology. 2017;7:1–4.
55. Chen S, Zhong X, Hu S, Dorn S, Kachelrieß M, Lell M, et al. Automatic multi-organ segmentation in dual-energy CT (DECT) with dedicated 3D fully convolutional DECT networks. Med Phys. 2020;47:552–62.
56. Homayounieh F, Singh R, Nitiwarangkul C, Lades F, Schmidt B, Sedlmair M, et al. Semiautomatic segmentation and radiomics for dual-energy CT: a pilot study to differentiate benign and malignant hepatic lesions. Am J Roentgenol. 2020; 215:398–405.
57. Seidler M, Forghani B, Reinhold C, Pérez-Lara A, Romero-Sanchez G, Muthukrishnan N, et al. Dual-energy CT texture analysis with machine learning for the evaluation and characterization of cervical lymphadenopathy. Comput Struct Biotechnol J. 2019;17:1009–15.
58. Zhu X, McCullough WP, Mecca P, Servaes S, Darge K. Dual-energy compared to single-energy CT in pediatric imaging: a phantom study for DECT clinical guidance. Pediatr Radiol. 2016;46:1671–9.
59. Tawfik AM, Kerl JM, Razek AA, Bauer RW, Nour-Eldin NE, Vogl TJ, et al. Image quality and radiation dose of dual-energy CT of the head and neck compared with a standard 120-kVp acquisition. AJNR Am J Neuroradiol. 2011;32:1994–9.
60. Suntharalingam S, Stenzel E, Wetter A, Guberina N, Umutlu L, Schlosser T, et al. Third generation dual-energy CT with 80/150 Sn kV for head and neck tumor imaging. Acta Radiol. 2019;60:586–92.
61. Tabari A, Gee MS, Singh R, Lim R, Nimkin K, Primak A, et al. Reducing radiation dose and contrast medium volume with application of dual-energy CT in children and young adults. Am J Roentgenol. 2020;214:1199–205.
62. Van Hamersvelt RW, Eijsvoogel NG, Mihl C, de Jong PA, Schilham AMR, Buls N, et al. Contrast agent concentration optimization in CTA using low tube voltage and dual-energy CT in multiple vendors: a phantom study. Int J Cardiovasc Imaging. 2018;34:1265–75.
63. Faggioni M, Mehran R. Preventing contrast-induced renal failure: A guide. Interv Cardiol Rev. 2016;11:98–104.
64. Raju R, Thompson AG, Lee K, Precious B, Yang TH, Berger A, et al. Reduced iodine load with CT coronary angiography using dual-energy imaging: a prospective randomized trial compared with standard coronary CT angiography. J Cardiovasc Comput Tomog. 2014;8:282–8.
65. Delesalle MA, Pontana F, Duhamel A, Faivre JB, Flohr T, Tacelli N, et al. Spectral optimization of chest CT angiography with reduced iodine load: experience in 80 patients evaluated with dual-source, dual-energy CT. Radiology. 2013; 267:256–66.
66. Shuman WP, O'Malley RB, Busey JM, Ramos MM, Koprowicz KM. Prospective comparison of dual-energy CT aortography using 70% reduced iodine dose versus single-energy CT aortography using standard iodine dose in the same patient. Abdom Radiol. 2017;42:759–65.
67. Lv P, Liu J, Chai Y, Yan X, Gao J, Dong J. Automatic spectral imaging protocol selection and iterative reconstruction in abdominal CT with reduced contrast agent dose: initial experience. Eur Radiol. 2017;27:374–83.
68. Tabari A, Gee MS, Singh R, Lim R, Nimkin K, Primak A, et al. Reducing radiation dose and contrast medium volume with application of dual-energy CT in children and young adults. Am J Roentgenol. 2020;214:1199–205.
69. Zhao Y, Geng X, Zhang T, Wang X, Xue Y, Dong K. Assessment of radiation dose and iodine load reduction in head-neck CT angiography using two scan protocols with wide-detector. J Xray Sci Technol. 2019;27:981–93.
70. Gibney B, Redmond CE, Byrne D, Mathur S, Murray N. A review of the applications of dual-energy CT in acute neuroimaging. Can Assoc Radiol J. 2020;71:253–65.
71. Blodgett TM, Fukui MB, Snyderman CH, Branstetter IVBF, McCook BM, Townsend DW, et al. Combined PET-CT in the head and neck: part 1. Physiologic, altered physiologic, and artifactual FDG uptake. Radiographics. 2005;25:897–912.
72. Ryan JL, Aaron VD, Sims JB. PET/MRI vs. PET/CT in head and neck imaging: when, why, and how? Sem Ultrasound CT MR. 2019;40:376–90.

73. Beckett KR, Moriarity AK, Langer JM. Safe use of contrast media: what the radiologist needs to know. Radiographics. 2015;35:1738–50.
74. Brennan KE, Hall SF, Owen TE, Griffiths RJ, Peng Y. Variation in routine follow-up care after curative treatment for head-and-neck cancer: a population-based study in Ontario. Curr Oncol. 2018;25:e120–31.
75. Willemink MJ, Persson M, Pourmorteza A, Pelc NJ, Fleischmann D. Photon-counting CT: technical principles and clinical prospects. Radiology. 2018;289:293–312.